Sugimoto *et al. Earth, Planets and Space* (2023) 75:44
https://doi.org/10.1186/s40623-023-01806-7

Earth, Planets and Space

EXPRESS LETTER

Open Access

# Super-rotation independent of horizontal diffusion reproduced in a Venus GCM

Norihiko Sugimoto[1*], Yukiko Fujisawa[1], Nobumasa Komori[1], Hiroki Kashimura[2,3], Masahiro Takagi[4] and Yoshihisa Matsuda[5]

**Abstract**

Horizontal diffusion and resolution are important factors to generate and maintain the super-rotation in the general circulation model (GCM) because waves which transport angular momentum are sensitive to them. Here, we investigated how the super-rotation depends on the magnitude of horizontal hyper diffusion using a Venus atmospheric GCM with medium and high resolutions. In both the runs, we found a parameter range where the structure of fully developed super-rotation is almost independent of the magnitude of horizontal diffusion. Spectral analysis shows that unrealistically strong super-rotation is developed when medium-scale disturbances are dissipated by stronger horizontal diffusion. On the other hand, artificially weak super-rotation is also realized because spurious small-scale disturbances are accumulated when the horizontal diffusion is too weak.

**Keywords** Venus atmosphere, Super-rotation, GCM, Horizontal diffusion

**Graphical Abstract**

Fully developed super-rotations reproduced in a Venus atmospheric GCM with medium (a) and high (b) resolutions are independent of the magnitude of horizontal diffusion. The appropriate magnitude of horizontal diffusion could be estimated by the spectral analysis (c).

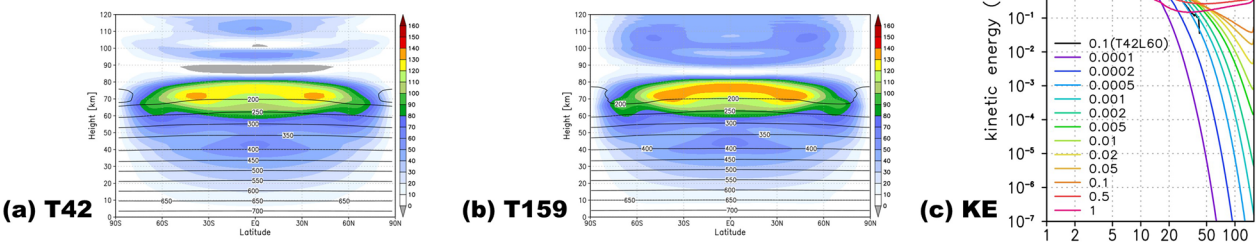


*Correspondence:
Norihiko Sugimoto
nori@phys-h.keio.ac.jp
Full list of author information is available at the end of the article

## Introduction

In the Venus atmosphere, fast zonal wind has been observed (e.g., Sánchez-Lavega et al. 2017; Read and Lebonnois 2018), which is called super-rotation, because it is much faster than the rotation period of the solid part of the planet. So far, Venus general circulation models (VGCMs) have been used to study the super-rotation and several studies obtained fully developed super-rotation faster than 100 m/s (e.g., Yamamoto and Takahashi 2003; Lee et al. 2005; Takagi and Matsuda 2007; Lebonnois et al. 2010; 2016). Sugimoto et al. (2019; hereafter STM2019) also reproduced fully developed super-rotation using a relatively high resolution VGCM named AFES-Venus (Sugimoto et al. 2014a), which is based on AFES (an atmospheric GCM for the Earth Simulator) (Ohfuchi et al. 2004), with weak vertical viscosity.

Recently, Yamamoto and Takahashi (2022; hereafter YT2022) pointed out that the super-rotation developed in their VGCM crucially depends on the magnitude of horizontal "hyper" diffusion, where "hyper" means that it is not normal Laplacian diffusion term of $\nabla^2(=\Delta)$. They suggested that the fully developed super-rotation obtained in STM2019 could be realized because strong horizontal diffusion was used in AFES-Venus. In the numerical simulation, it is desirable to set the magnitude of horizontal diffusion to be as weak as possible within the range where the energy is not accumulated at the maximum wavenumber. In AFES-Venus, the second-order horizontal hyper diffusion (Laplacian squared, $\Delta^2 = \nabla^4$) is used and the damping times for the maximum wavenumber component are determined by the spectral analysis. For example, the damping times are 0.1 Earth days for T42L60 (Sugimoto et al. 2014a; Ando et al. 2016; STM2019), 0.03–0.05 Earth days for T63L120 (Sugimoto et al. 2014b; Takagi et al. 2018), 0.01 Earth day for T159L120 (Kashimura et al. 2019), and 0.0003 Earth days for T639L260 (Sugimoto et al. 2021) runs, where T and L denote the triangular truncation number for spherical harmonics and vertical levels, respectively. These values are comparable to those used in the Earth GCM (MIROC; Model for Interdisciplinary Research on Climate) (K-1 model developers 2004). YT2022, however, used very weak horizontal diffusion (the relaxation times are more than one Earth day for T42L50 runs) and then the super-rotation was not fully developed. Furthermore, they did not propose an appropriate damping rate.

In the present study, we examine how the super-rotation depends on the magnitude of horizontal diffusion and propose the appropriate damping rate clearly by the spectral analysis. The fully developed super-rotation is maintained for both the medium (T42L60) and high (T159L120) resolution runs in a same range of the magnitude of horizontal diffusion. Note that since horizontally smaller disturbances tend to have smaller vertical scales, it is usual to increase the vertical resolution according to the horizontal resolution; though the increasing rates are usually not equal due to computational cost. Although we did not conduct sensitivity experiments on the vertical resolution, we have confirmed that there is no significant change in the atmospheric structures of T42L60 (Sugimoto et al. 2014a; Ando et al. 2016; STM2019), T42L120 (Ando et al. 2020), T63L120 (Sugimoto et al. 2014b; Ando et al. 2018; Takagi et al. 2018), T159L120 (Kashimura et al. 2019), and T639L260 (Sugimoto et al. 2021) runs.

## Experimental setup

AFES-Venus is a spectral GCM for the Venus atmosphere solving nonlinear primitive equations on a sphere (Sugimoto et al. 2014a). The truncation wavenumbers are 42 for medium resolution runs (T42L60) and 159 for high resolution runs (T159L120), then the numbers of horizontal grids are $128 \times 64$ and $480 \times 240$ for the T42L60 and T159L120 resolutions, respectively. The atmosphere is divided into 60 and 120 levels from the ground to ~ 120 km at regular spacings of 2 and 1 km in height for the T42L60 and T159L120 resolutions, respectively. The vertical eddy viscosity is included and its coefficient is fixed to 0.0015 $m^2/s$ to maintain the super-rotation (STM2019). The horizontal eddy diffusion is the same as STM2019, which is represented by the second-order horizontal hyper diffusion (Laplacian squared, $\Delta^2 = \nabla^4$). For the sensitivity experiments, its damping time for the maximum wavenumber component is swept through 10 values (0.01, 0.05, 0.1, 0.2, 0.5, 1, 2, 5, 10, 30 Earth days) for T42L60 runs and 12 values (0.0001, 0.0002, 0.0005, 0.001, 0.002, 0.005, 0.01, 0.02, 0.05, 0.1, 0.5, 1 Earth day(s)) for T159L120 runs. Note that because the strength of horizontal diffusion is expressed by the damping time for the maximum wavenumber component, the horizontal diffusion coefficient is about $4^4 = 256$ times larger in T42L60 than that in T159L120 when the same value is set for the damping time (see Additional file 1: S1); also note that, in this paper, the word "damping time" is always used to indicate that for the maximum wavenumber component. Rayleigh friction is used as the surface friction at the lowest level and its relaxation time is set to 0.5 Earth days. A sponge layer is applied only to eddy components above 80 km and its coefficient gradually increases with height.

The solar heating is based on Tomasko et al. (1980). In contrast to the previous studies STM2019 and YT2022, the thermal tides are excited in the present model because its diurnal component is included. The infrared radiative process is simplified by the Newtonian cooling with relaxation time based on Crisp (1989). A

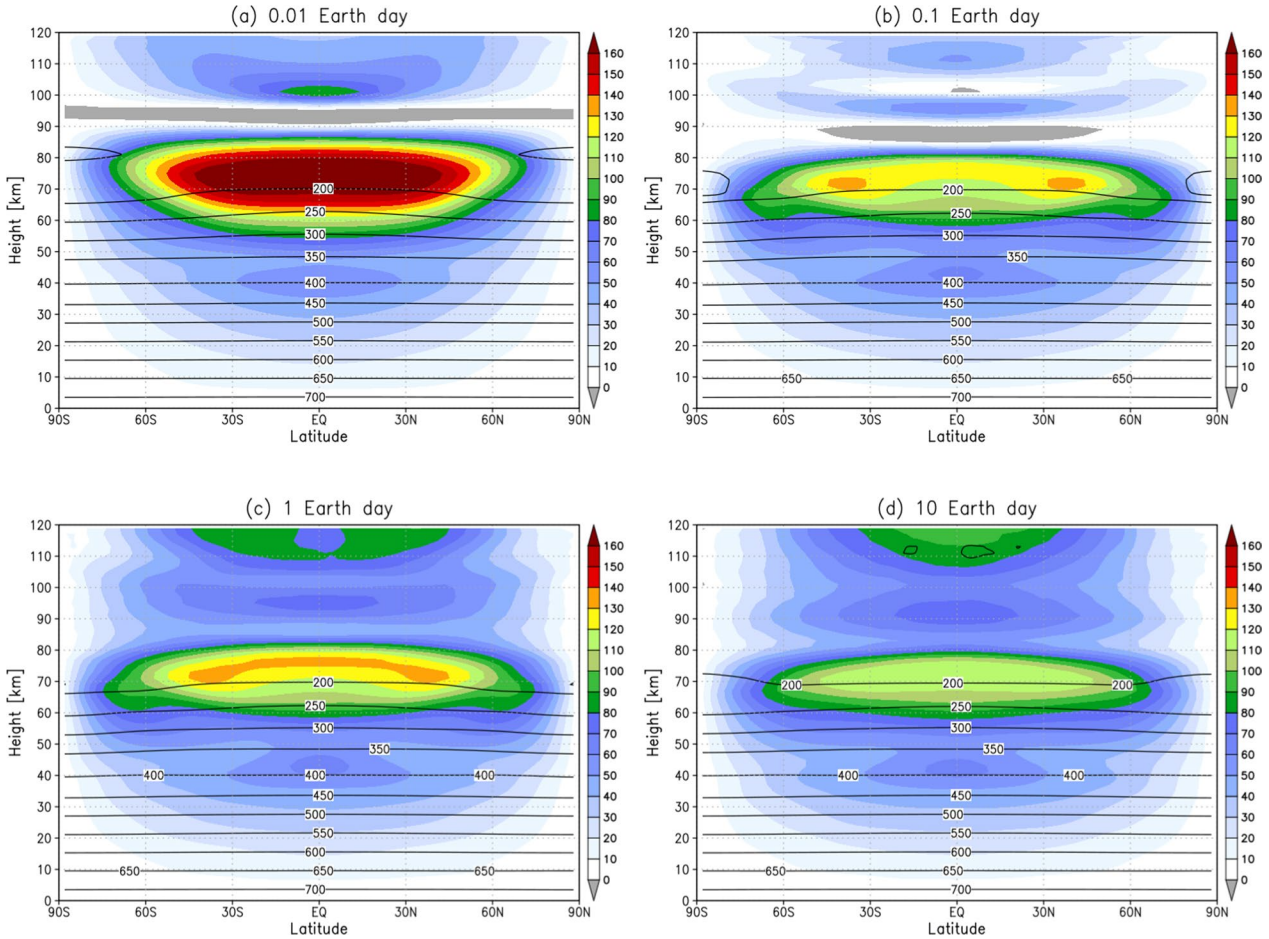


**Fig. 1** Zonal-mean zonal flow (colour, m/s) and temperature (contour, K) obtained for T42L60 run. Latitude–height cross sections for the cases with **a** 0.01, **b** 0.1, **c** 1, and **d** 10 Earth days for the damping time of horizontal diffusion are shown. They are temporally averaged over the last 1 Earth year (360 datasets of daily data)

horizontally uniform temperature field, which is based on VIRA (Venus international reference atmosphere, Seiff et al. 1985) and observed static stability (Tellmann et al. 2009) with a weakly stratified layer extending from 55 to 60 km, is used as a relaxation field of the Newtonian cooling. The initial condition is an idealized super-rotating flow in solid-body rotation. At the equator the zonal flow increases to 100 m/s linearly with height from the ground to 70 km. Above 70 km it is constant. The horizontal distribution of temperature field is in gradient wind balance with this zonal flow. From this initial state, nonlinear numerical simulations are conducted for 4 Earth years. The model output is sampled at every 1 Earth day (24 h). Note that AFES-Venus has realistically reproduced the super-rotation with planetary-scale waves (Sugimoto et al. 2014b; Takagi et al. 2022), polar vortex with cold collar (Ando et al. 2016, 2017), thermal tides (Takagi et al. 2018; Suzuki et al. 2022), thermal structure in equatorial region (Ando et al. 2018), and planetary-scale streak structure (Kashimura et al. 2019) by the similar settings of this study. The directions of planetary rotation and basic zonal flow are set to be eastward (positive) in the present study. Details of experimental settings are described in Sugimoto et al. (2014a, b).

## Results

Figure 1 shows zonal-mean zonal flow and temperature in a latitude–height cross section for the cases with (a) 0.01, (b) 0.1, (c) 1, and (d) 10 Earth days for the damping time of horizontal diffusion obtained for T42L60 run (see also Additional file 1: S2 (Figure S1) for the cases with 0.05, 0.2, 0.5, 2, 5, and 30 Earth days). They are temporally averaged over the last 1 Earth year (360 datasets of daily data). The fully developed super-rotation of ~ 130 m/s with mid-latitude jets appears at ~ 70 km for the cases with moderate damping time (0.1 and 1 Earth day(s)) of horizontal diffusion (Fig. 1b, c); these super-rotational flows are similar to those obtained in the previous studies

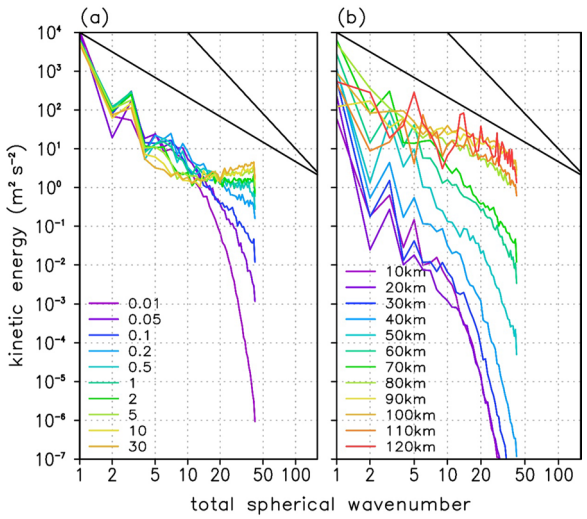


**Fig. 2** Kinetic energy of horizontal wind per unit mass per unit wavenumber for T42L60 run. **a** Dependency on the damping time of horizontal diffusion at 70 km. **b** Dependency on the height for the case with 0.1 Earth days for the damping time of horizontal diffusion. Gradient of $n^{-5/3}$ and $n^{-3}$ are shown by solid lines. The analysed data is the final day of the numerical simulation

(Sugimoto et al. 2014b; Takagi et al. 2018) and consistent with observations (e.g. Machado et al. 2012). For the case with stronger horizontal diffusion (0.01 Earth days), the faster super-rotation of ~ 180 m/s without mid-latitude jets appears (Fig. 1a). For the case with weaker horizontal diffusion (10 Earth days), the slower super-rotation of ~ 110 m/s without mid-latitude jets appears. These results are qualitatively consistent with that shown in YT2022. Because the super-rotation is very similar between the two cases with 10 times different magnitude of horizontal diffusion (Fig. 1b, c), it is suggested that the super-rotation is maintained by the resolved eddies and the dependence on unresolved eddies (i.e., horizontal diffusion) is negligible in this range.

In order to check the accumulation of spurious small-scale disturbances, the spectral analysis of kinetic energy of horizontal wind is performed for T42L60 run. Figure 2a shows how it depends on the damping time of horizontal diffusion at 70 km. It is clearly seen that the spectra in large-scales (with total wavenumber less than 5) are almost unchanged for the cases with moderate damping time (from 0.1 to 2 Earth days). For the cases with stronger horizontal diffusion (0.01 (orchid) and 0.05 (purple) Earth days), the spectra in small-scales decrease with total wavenumber quite rapidly and those in large-scales are smaller than those obtained for the moderate horizontal diffusion. For the cases with weaker horizontal diffusion (5 (lime green), 10 (khaki), and 30 (mocha) Earth days), the spectra in small-scales increase with total wavenumber, indicating the accumulation of spurious small-scales. The spectra in large-scales (with total wavenumber 2 and 3) are also smaller than those obtained for the moderate horizontal diffusion.

Figure 2b shows how the kinetic energy of horizontal wind depends on height of for the case with the moderate damping time (0.1 Earth days) of horizontal diffusion. Though the spectral slope in small-scales tend to be shallower above 80 km because of wave propagation from 60 to 70 km altitudes (the upper cloud layer), the accumulation of spurious small-scales does not occur. For weaker horizontal diffusion (with the damping time longer than 0.2 Earth days), the accumulation of spurious small-scales occurs in the upper atmosphere above 80 km even though the obtained super-rotation is similar in each case at the cloud top level. This result suggests that influence of the accumulation of the kinetic energy in small-scales above 80 km might be cancelled out by the sponge layer. However, to be on the safer side, we used 0.1 Earth days for the damping time of horizontal diffusion for T42L60 run in Sugimoto et al. (2014a) and STM2019.

Usually, results obtained with lower resolutions are validated by those with higher resolutions. Figure 3 shows zonal-mean zonal flow and temperature in a latitude–height cross section for the cases with (a) 0.0001, (b) 0.001, (c) 0.01, (d) 0.1, and (e) 1 Earth day(s) for the damping time of horizontal diffusion obtained for T159L120 high resolution run. They are again temporally averaged over the last 1 Earth year (360 datasets of daily data). The fully developed super-rotation of ~ 130 m/s with mid-latitudes jets appears at ~ 70 km for the cases with a wide range of damping time (from 0.001 to 0.1 Earth days) of horizontal diffusion (Fig. 3b–d), which is very similar to those obtained for T42L60 run with the moderate damping time (0.1 and 1 Earth day(s)) of horizontal diffusion (Fig. 1b, c). For the case with stronger horizontal diffusion (0.0001 Earth days), the faster super-rotation of ~ 160 m/s without mid-latitude jets appears (Fig. 3a). For the case with weaker horizontal diffusion (1 Earth day), the slower super-rotation of ~ 100 m/s without mid-latitude jets appears. These results are also consistent with that obtained for T42L60 run. Again, because the super-rotation is very similar among the cases in a very wide parametric range of the horizontal diffusion strength with different resolutions of T159L120 (Fig. 3b–d) and T42L60 (Fig. 1b, c), it is strongly suggested that the super-rotation is maintained by the resolved eddies and the dependence on horizontal diffusion is negligible in this range.

The spectral analysis of kinetic energy is also performed for T159L120 run. Figure 4a shows its dependency on the damping time of horizontal diffusion at 70 km.

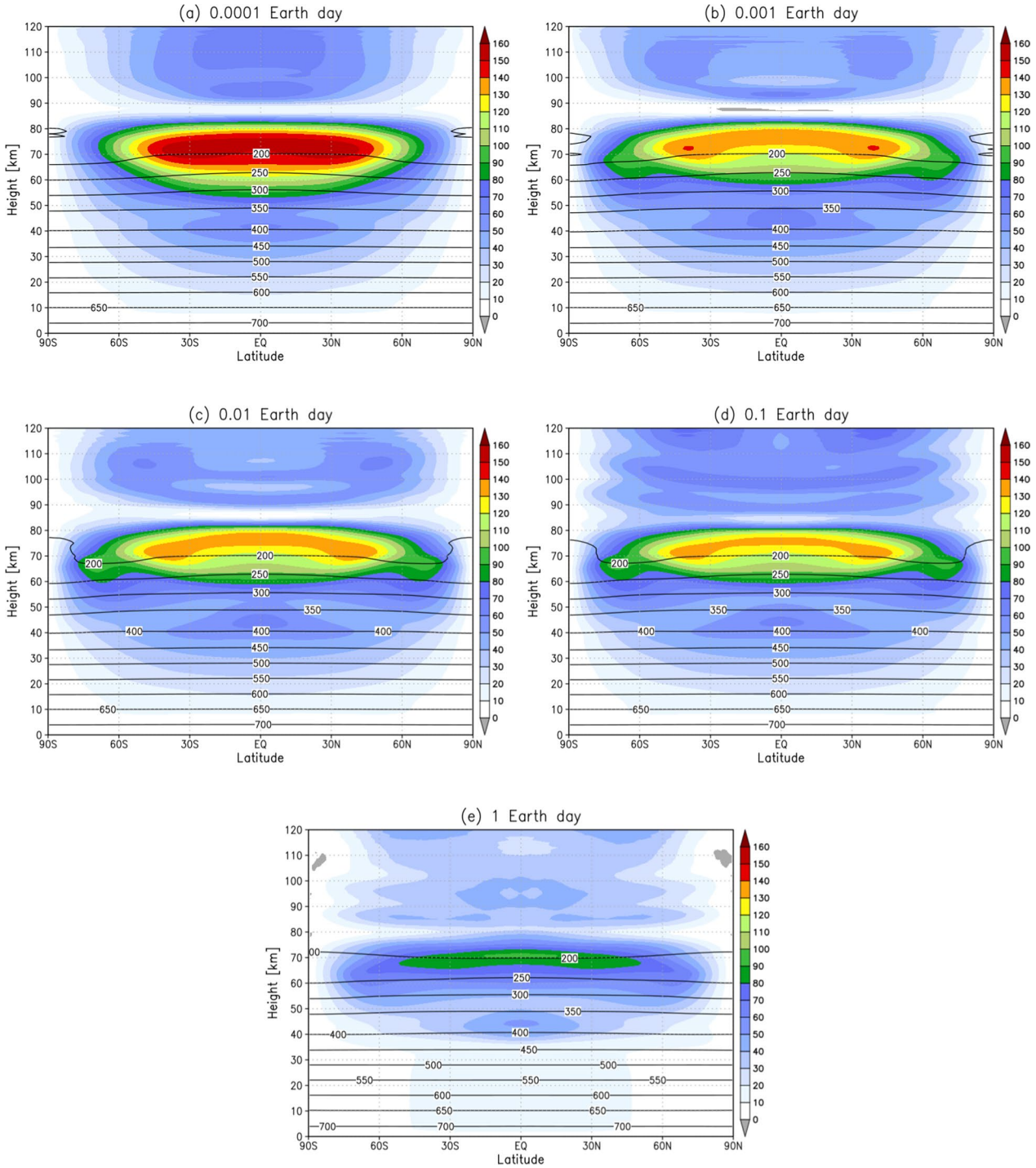


**Fig. 3** Zonal-mean zonal flow (colour, m/s) and temperature (contour, K) obtained for T159L120 run. Latitude–height cross sections for the cases with **a** 0.0001, **b** 0.001, **c** 0.01, **d** 0.1, and **e** 1 Earth day(s) for the damping time of horizontal diffusion are shown. They are temporally averaged over the last 1 Earth year (360 datasets of daily data)

It is clearly seen that for the cases with a wide range of moderate damping time (from 0.0005 to 0.1 Earth days) of horizontal diffusion, the spectra in large- and medium-scales (with total wavenumber less than 20) are almost unchanged among the cases and similar to those obtained in T42L60 run with a damping time of 0.1

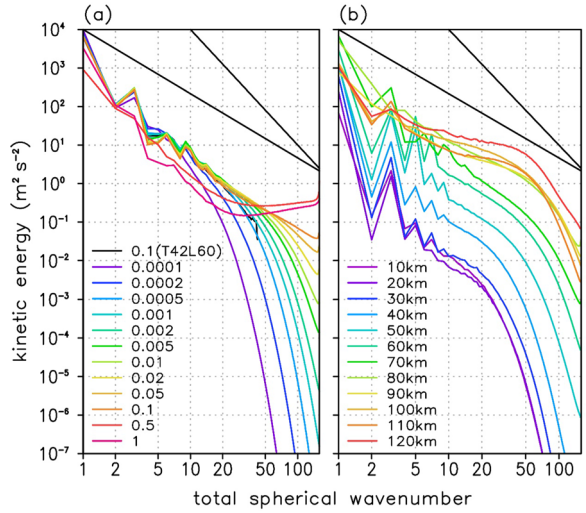


**Fig. 4** Kinetic energy of horizontal wind per unit mass per unit wavenumber for T159L120 run. **a** Dependency on the damping time of horizontal diffusion at 70 km. **b** Dependency on the height for the case with 0.01 Earth days for the damping time of horizontal diffusion. Gradient of $n^{-5/3}$ and $n^{-3}$ are shown by solid lines. They are temporally averaged over the last 1 Earth year (360 datasets of daily data)

Earth days (black) of horizontal diffusion. For the cases with stronger horizontal diffusion (0.0001 (purple) and 0.0002 (blue) Earth days), the spectra rapidly decrease with total wavenumber more than 10. For the cases with weaker horizontal diffusion (0.5 (orange) and 1 (pink) Earth day(s)), the spectra in small-scales increase with total wavenumber, indicating the accumulation of spurious small-scales. The spectra in large-scales (with total wavenumber less than 10) are also smaller than those with the moderate horizontal diffusion. Figure 4b shows the dependency of kinetic energy on height for the case with the moderate damping time (0.01 Earth days) of horizontal diffusion. Though the spectral slope in small-scales tend to be shallower above 80 km because of the wave propagation from the upper cloud layer (from 60 to 70 km), the accumulation of spurious small-scales does not occur, as in T42L60 run. For weaker horizontal diffusion (larger than 0.02 Earth days), even though the super-rotation is similar in each case at the cloud top level, the accumulation of spurious small-scales occurs in the upper atmosphere above 80 km. With the same reason mentioned above for previous studies with the T42L60 resolution, we used 0.01 Earth days for the damping time of horizontal diffusion for T159L120 resolution in Kashimura et al. (2019).

Finally, zonal wind deviation (color, m/s) from its zonal mean at 70 km is shown in a longitude–latitude cross section for the cases with (a) 0.01, (b) 0.1, (c) 1, and (d) 10 Earth days of the damping time of horizontal diffusion obtained for T42L60 run (Fig. 5). In all the cases, the diurnal (semi-diurnal) tide with wavenumber 1 (2) in the mid- to high-latitudes (low-latitude) are predominant. For the case with moderate horizontal diffusion (0.1 Earth days), there are also medium-scale disturbances (Fig. 5b). However, for the case with stronger horizontal diffusion (0.01 Earth days), only the large-scale structure can be seen; this indicates that disturbances of medium-scales are dissipated or decreased by the horizonal diffusion (Fig. 5a). For the cases with weaker horizontal diffusion (1 and 10 Earth days; Fig. 5c, d), small-scale disturbances appear randomly, reflecting the accumulation of the kinetic energy in the smallest scales shown by magenta and purple lines in Fig. 2a.

## Summary and discussion

In the present study, we investigated how the super-rotation depends on the magnitude of horizontal diffusion using AFES-Venus (atmospheric general circulation model for the Earth Simulator for Venus) with medium (T42L60) and high (T159L120) resolutions. For a range of the magnitude of horizontal diffusion (from 0.1 to 1 Earth days for T4260 and from 0.0005 to 0.1 Earth days for T159L120 runs, respectively), fully developed super-rotation was obtained for several cases in both the resolutions, which is almost independent of the magnitude of horizontal diffusion and similar among these cases. For the cases with stronger horizontal diffusion, unrealistically strong super-rotation was developed and medium-scale disturbances are vanished. It is suggested that equatorward momentum transport caused by strong horizontal hyper diffusion can produce the strong super-rotation artificially, namely, Gierasch-Rossow-Williams mechanism (Gierasch 1975; Rossow and Williams 1979) works too much in these cases. For the cases with weaker horizontal diffusion, weak super-rotation was artificially realized and the accumulation of spurious small-scale disturbances occurred. It seems that spurious small-scale disturbances and inverse cascades from small-scales work to weaken the super-rotation and this effect is larger than that of resolved disturbances which contribute to the maintenance of super-rotation. Therefore, the results strongly suggested that the damping rate of 0.1 Earth days for the horizontal diffusion in T42L60 is reasonable and disturbances is resolved to maintain the super-rotation for that value.

Remember that we have expressed the strength of horizontal diffusion (represented by the second-order Laplacian) by the damping time for the maximum wavenumber component of the resolution setting. The value of horizontal diffusion coefficient that corresponds to the damping time of 0.1 Earth days for the horizontal wavenumber

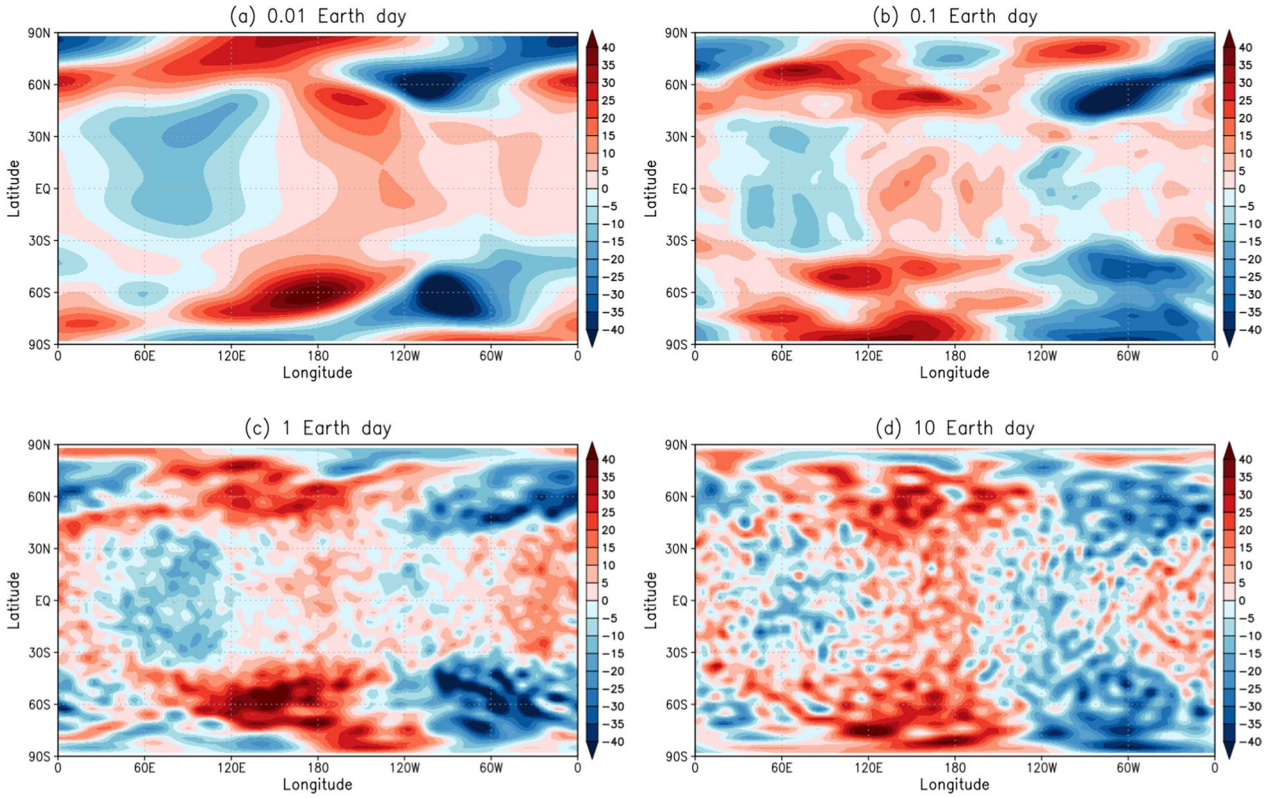


**Fig. 5** Zonal wind disturbances (color, m/s) from its zonal mean obtained for T42L60 run. Longitude–latitude cross sections at 70 km for the cases with **a** 0.01, **b** 0.1, **c** 1, and **d** 10 Earth days of the damping time of horizontal diffusion are shown. The analysed data is the final day of the numerical simulation

42 (in Venus) is $\sim 4.8 \times 10^{16}$ $m^4/s$ (see Additional file 1: S4). With this coefficient value, the damping time for the wavenumber 159 is ~ 0.0005 Earth days. The reproduced super-rotation in T42L60 run with the damping time of 0.1 Earth days could be verified by T159L120 run with the damping time of 0.0005 Earth days (Figure S2a) and it is also confirmed that the two spectra match very well in the spectral analysis (Fig. 4a; black and blue lines). Similarly, the magnitude of horizontal diffusion with the damping time of 10 Earth days for the case of T42L60 is comparable to that with ~ 0.05 Earth days for the case of T159L120. However, since the reproduced super-rotation in T42L60 run is totally different from that reproduced in the cases of T159L120 run, T42L60 run with the damping time of 10 Earth days cannot be reliable.

Similarity of the obtained super-rotation with different resolutions (T42L60 and T159L120) and different strength of horizontal diffusion suggests that disturbances smaller than ~ 900 km is less important at least for maintaining the super-rotation. Although the slope of the energy spectra is out of focus in the present study, there seems to be a region of energy cascade with −5/3 slope for total wavenumber less than ~ 20 (~ 50) in T42L60 (T159L120) runs, which is consistent with that for the Earth (Takahashi et al. 2006). It is also well known that the direct energy cascade from large-scales of motion (quasi-2D flow) to small-scales with −3 slope (Nastrom and Gage 1985) in larger scales, though it is difficult to find such kind of slope in Figs. 2 and 4. In conclusion, we should carefully check the magnitude of horizontal diffusion by the spectral analysis and higher resolution runs before conducting the long-term Venus GCM simulations to reproduce the super-rotation.

**Abbreviations**

| | |
|---|---|
| GCM | General circulation model |
| VGCM | Venus general circulation model |
| AFES | Atmospheric GCM for the Earth Simulator |
| MIROC | Model for Interdisciplinary Research On Climate |
| VIRA | Venus international reference atmosphere |

## Supplementary Information

The online version contains supplementary material available at https://doi.org/10.1186/s40623-023-01806-7.

**Additional file 1.** Explanation of Supplementary Information and additional figures.

**Additional file 2.** Data set.

**Acknowledgements**
This study was conducted under the joint research project of the Earth Simulator with title "High resolution general circulation simulation of Venus and Mars atmosphere using AFES". The GFD-DENNOU Library was used for creating figures. The authors thank two anonymous reviewers for useful comments.

**Author contributions**
NS designed the study and analyzed the data with a help of YF, NK, and HK. NS wrote the manuscript. All authors discussed the contents of the study. All authors read and approved the final manuscript.

**Funding**
The work is partly supported by JSPS KAKENHI Grants Numbers JP19H01971, JP19H05605, JP20K04062, and JP20K04064. This work is also supported by JST FOREST Program (Grant Number JPMJFR212R, Japan).

**Availability of data and materials**
Results from the GCM simulations performed in this paper are provided as supplementary information (Additional file 2).

## Declarations

**Ethics approval and consent to participate**
Not applicable.

**Consent for publication**
Not applicable.

**Competing interests**
The author declares that they have no competing interests.

**Author details**
[1]Research and Education Center for Natural Sciences, Department of Physics, Keio University, Yokohama 223-8521, Japan. [2]Department of Planetology, Kobe University, Kobe 657-8501, Japan. [3]Center for Planetary Science, Kobe University, Kobe 650-0047, Japan. [4]Faculty of Science, Kyoto Sangyo University, Kyoto 603-8555, Japan. [5]Department of Astronomy and Earth Science, Tokyo Gakugei University, Koganei 184-8501, Japan.

Received: 18 December 2022 Accepted: 10 March 2023
Published online: 24 March 2023

**References**

Ando H, Sugimoto N, Takagi M, Kashimura H, Imamura T, Matsuda Y (2016) The puzzling Venusian polar atmospheric structure reproduced by a general circulation model. Nat Commun 7:10398. https://doi.org/10.1038/ncomms10398

Ando H, Imamura T, Sugimoto N, Takagi M, Kashimura H, Tellmann S, Pätzold M, Häusler B, Matsuda Y (2017) Vertical structure of the axi-asymmetric temperature disturbance in the Venusian polar atmosphere: Comparison between radio occultation measurements and GCM results. J Geophys Res Planets 122:1687–1703. https://doi.org/10.1002/2016JE005213

Ando H, Takagi M, Fukuhara T, Imamura T, Sugimoto N, Sagawa H et al (2018) Local time dependence of the thermal structure in the Venusian equatorial upper atmosphere: Comparison of Akatsuki radio occultation measurements and GCM results. J Geophys Res Planets 123:2270–2280. https://doi.org/10.1029/2018JE005640

Ando H, Takagi M, Sugimoto N, Sagawa H, Matsuda Y (2020) Venusian cloud distribution simulated by a general circulation model. J Geophys Res Planets. https://doi.org/10.1029/2019JE006208

Crisp D (1989) Radiative forcing of the Venus mesosphere. II. Thermal fluxes, cooling rates, and radiative equilibrium temperatures. Icarus 77:391–413. https://doi.org/10.1016/0019-1035(89)90096-1

Gierasch PJ (1975) Meridional circulation and the maintenance of the Venus atmospheric rotation. J Atmos Sci 32(6):1038–1044. https://doi.org/10.1175/1520-0469(1975)032%3C1038:MCATMO%3E2.0.CO;2

K-1 model developers (2004). In Hasumi, H. and Emori, S. (Eds.), K-1 coupled GCM (MIROC) description, K-1 Tech. Rep. (Vol. 1, p. 34). Japan: Center for Climate System Research, the University of Tokyo.

Kashimura H, Sugimoto N, Takagi M, Ohfuchi W, Enomoto T, Nakajima K et al (2019) Planetary-scale streak structure reproduced in a Venus atmospheric simulation. Nat Commun 10:23. https://doi.org/10.1038/s41467-018-07919-y

Lebonnois S, Hourdin F, Eymet V, Crespin A, Fournier R, Forget F (2010) Superrotation of Venus' atmosphere analyzed with a full general circulation model. J Geophys Res Planets 115:E06006. https://doi.org/10.1029/2009JE003458

Lebonnois S, Sugimoto N, Gilli G (2016) Wave analysis in the atmosphere of Venus below 100 km altitude, simulated by LMD Venus GCM. Icarus 278:38–51. https://doi.org/10.1016/j.icarus.2016.06.004

Lee C, Lewis SR, Read PL (2005) A numerical model of the atmosphere of Venus. Adv Space Res 36:2142–2145. https://doi.org/10.1016/j.asr.2005.03.120

Machado P, Luz D, Widemann T, Lellouch E, Witasse O (2012) Mapping zonal winds at Venus's cloud tops from ground-based Doppler velocimetry. Icarus 221:248–261. https://doi.org/10.1016/j.icarus.2012.07.012

Nastrom GD, Gage KS (1985) A Climatology of Atmospheric Wavenumber Spectra of Wind and Temperature Observed by Commercial Aircraft. J Atmos Sci 42(9):950–960. https://doi.org/10.1175/1520-0469(1985)042%3c0950:ACOAWS%3e2.0.CO;2

Ohfuchi W, Nakamura H, Yoshioka MK, Enomoto T, Takaya K, Peng X, Yamane S, Nishimura T, Kurihara Y, Ninomiya K (2004) 10-km Mesh Meso-scale Resolving Simulations of the Global Atmosphere on the Earth Simulator, -Preliminary Outcomes of AFES (AGCM for the Earth Simulator)-. J Earth Simulator 1:8–34. https://doi.org/10.32131/jes.1.8

Read PL, Lebonnois S (2018) Superrotation on Venus, on Titan, and Elsewhere. Annu Rev Earth Planet Sci 46:175–202. https://doi.org/10.1146/annurev-earth-082517-010137

Rossow WB, Williams GP (1979) Large scale motions in the Venus stratosphere. J Atmos Sci 36(3):377–389. https://doi.org/10.1175/1520-0469(1979)036%3C0377:LSMITV%3E2.0.CO;2

Sánchez-Lavega A, Lebonnois S, Imamura T, Read P, Luz D (2017) The Atmospheric Dynamics of Venus. Space Sci Rev 212:1541–1616. https://doi.org/10.1007/s11214-017-0389-x

Seiff A, Schofield JT, Kliore AJ, Taylor FW, Limaye SS, Revercomb HE et al (1985) Models of the structure of the atmosphere of Venus from the surface to 100 kilometers altitude. Adv Space Res 5:3–58. https://doi.org/10.1016/0273-1177(85)90197-8

Sugimoto N, Takagi M, Matsuda Y (2014a) Baroclinic instability in the Venus atmosphere simulated by GCM. J Geophys Res Planets 119:1950–1968. https://doi.org/10.1002/2014JE004624

Sugimoto N, Takagi M, Matsuda Y (2014b) Waves in a Venus general circulation model. Geophys Res Lett 41:7461–7467. https://doi.org/10.1002/2014GL061807

Sugimoto N, Takagi M, Matsuda Y (2019) Fully developed super-rotation driven by the mean meridional circulation in a Venus GCM. Geophys Res Lett 46:1776–1784. https://doi.org/10.1029/2018GL080917

Sugimoto N, Fujisawa Y, Kashimura H, Noguchi K, Kuroda T, Takagi M, Hayashi Y-Y (2021) Generation of gravity waves from thermal tides in the Venus atmosphere. Nat Commun 12:3682. https://doi.org/10.1038/s41467-021-24002-1

Suzuki A, Takagi M, Ando H, Imai M, Sugimoto N, Matsuda Y (2022) A sensitivity study of the thermal tides in the Venusian atmosphere: Structures and dynamical effects on the superrotation. J Geophys Res Planets 127:e2022JE007243. https://doi.org/10.1029/2022JE007243

Takagi M, Matsuda Y (2007) Effects of thermal tides on the Venus atmospheric superrotation. J Geophys Res 112:D09112. https://doi.org/10.1029/2006JD007901

Takagi M, Sugimoto N, Ando H, Matsuda Y (2018) Three dimensional structures of thermal tides simulated by a Venus GCM. J Geophys Res Planets 123:335–352. https://doi.org/10.1002/2017JE005449
Takagi M, Ando H, Sugimoto N, Matsuda Y (2022) A GCM Study on the 4-Day and 5-Day Waves in the Venus Atmosphere. J Geophys Res Planets 127:e2021JE007164. https://doi.org/10.1029/2021JE007164
Takahashi YO, Hamilton K, Ohfuchi W (2006) Explicit global simulation of the mesoscale spectrum of atmospheric motions. Geophys Res Lett 33:L12812. https://doi.org/10.1029/2006GL026429
Tellmann S, Pätzold M, Häusler B, Bird MK, Tyler GL (2009) Structure of the Venus neutral atmosphere as observed by the Radio Science experiment VeRa on Venus Express. J Geophys Res 114:E00B36. https://doi.org/10.1029/2008JE003204
Tomasko MG, Doose LR, Smith PH, Odell AP (1980) Measurement of the flux of sunlight in the atmosphere of Venus. J Geophys Res 85:8167–8186. https://doi.org/10.1029/JA085iA13p08167
Yamamoto M, Takahashi M (2003) Superrotation and equatorial waves in a T21 Venus-like AGCM. Geophys Res Lett 30(9):1449. https://doi.org/10.1029/2003GL016924
Yamamoto M, Takahashi M (2022) Sensitivities of general circulation and waves to horizontal subgrid-scale diffusion in long-term time integrations of a dynamical core for Venus. J Geophys Res Planets 127:e2022JE007209. https://doi.org/10.1029/2022JE007209

## Publisher's Note